JOURNAL OF Materials CHEMISTRY

# Ferroelectric cyclic oligosiloxane liquid crystals

**David R. Medeiros, Michael A. Hale, Raymond J. P. Hung, Jeffrey K. Leitko and C. Grant Willson***

*Departments of Chemistry and Chemical Engineering, University of Texas at Austin, Austin, TX 78712, USA*

***Received 18th December 1998, Accepted 9th April 1999***

Chiral, smectogenic pendant groups have been covalently attached to cyclic oligosiloxanes by hydrosilylation. These materials and the olefinic compounds from which they were derived exhibit ferroelectric behavior. The mesomorphic range, and in particular the $S_C$* phase, of these oligomers is greatly enhanced relative to the vinylogous parents. The electro-optic and thermal properties, in addition to the synthetic procedures used to prepare these materials, are described in detail. These compounds are seen as potential precursors to liquid crystalline polymers with desirable processing capabilities.

## Introduction

Researchers have been able to marry the attractive film forming and mechanical properties of polymers with the many useful anisotropic properties of liquid crystals (LC's) by covalently attaching pendant groups that impart liquid crystalline behavior onto polymer backbones. Polymeric LC's are particularly applicable for use in display devices. Numerous reports of research on the extension of electrooptic LC behavior into macromolecular systems have been made in the past two decades.[1–5] Recently, this approach has been expanded to include examples with $S_C$* LC's that exhibit ferroelectric and electroclinic switching.[6–12]

One limitation of LC polymers, particularly with respect to their use for fast electrooptic switching, is their higher viscosity. Poly(siloxanes) are relatively low viscosity liquids or greases at ambient temperatures, and therefore have been explored as a potential answer to this dilemma.[4–13] In particular, incorporation of low molar mass ferroelectric liquid crystals onto poly(siloxanes) has been shown to have the additional benefit of enhancing the temperature range at which LC phases occur.[4,5,7,10,14] Furthermore, recent reports of cyclic siloxane oligomers with LC pendant groups have shown that these materials exhibit properties intermediate to low molecular mass and polymeric LC's.[4,5,13,15–17] Previous work by Gray, Goodby, Zentel and others demonstrates a variety of structural variations on this theme and provides much insight into the characteristics of materials in this intermediate class of macromolecular LC's.[4,5,18–20] Specifically, these materials maintain the switching speed and high polarization of the monomeric compounds while allowing for enhanced processability. It is generally necessary to rely on the flow of the isotropic melts of low molecular mass materials to fill electrode cells, but polymeric LC materials and cyclic siloxane LC oligomers have been shown to form high quality films upon spin casting from solvents.[13]

Since cyclic siloxanes can undergo ring opening polymerization in the presence of an acid catalyst,[5,21,22] it may be possible to use these materials as precursors to poly(siloxanes). The cyclic oligomers are attractive from a synthetic point of view as they are discrete, well-defined molecules that are suitable for isolation and purification by conventional techniques used for low molecular mass compounds. The polymeric counterparts are distributions of different size macromolecules that may vary in their degree of functional group substitution and end-group identity. Once isolated, *in situ* polymerization by photochemically generated acid is envisioned as a means of further manipulating the properties of this system by providing a means of 'locking-in' electrooptic properties after alignment or orientation is achieved in the more fluid state of the oligomers.[22] Macroscopic optical and dielectric anisotropy could thus be generated in thin films, allowing for an extension in the utility of these compounds in fast electrooptic devices.

A family of cyclic oligomeric siloxanes possessing pendant mesogenic groups has been prepared and their polymorphism and electrooptic properties have been investigated. A schematic representation of these compounds is shown in Fig. 1. The length of the tethering alkyl chain was varied and is noted in the labels for each oligomer (**O-#**). The precursors to these oligomers are interesting low molecular mass LC's in their own right. These compounds (**M-#**) consist of the same structural components of some previously reported materials,[23] including the laterally linked dimers presented earlier,[24] but differ by having terminal olefinic groups. This allows mesogen attachment to hydrosiloxane oligomers with a transition metal catalyst. The synthesis of these compounds and an evaluation of the mesomorphic and electrooptic properties of both the monomers and cyclic oligomers are presented in this report.

## Experimental

### General

All chemicals were purchased from Aldrich and were used as received unless otherwise noted. Solvents were distilled by conventional methods prior to use. Merck silica gel (9385 grade, 230–400 mesh, 60 Å) was used for all column chromatography separations.

$^1$H NMR (500 MHz) spectra were collected on a Varian

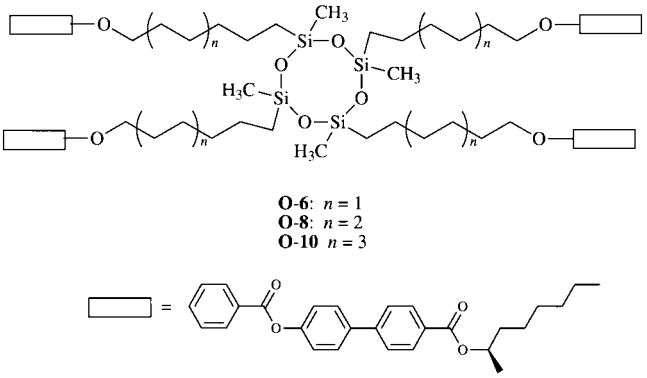

**O-6**: $n = 1$
**O-8**: $n = 2$
**O-10** $n = 3$



**Fig. 1** General structure of cyclic siloxane oligomers with pendant smectogens.

HMQC spectrometer. FTIR spectra were measured with a Nicolet Magna-IR spectrometer. Specific rotations were calculated from observed rotations measured in methylene chloride on a Perkin Elmer 241-MC polarimeter. Mass spectra were measured using a Finnigan MAT TSQ-70 spectrometer. Elemental analyses were performed by Galbraith Laboratories. DSC measurements were made on a Perkin Elmer Series-7 calorimeter. A scan rate of 5 °C $min^{-1}$ was used for all DSC analyses.

Equipment and techniques used to perform electrooptic measurements of spontaneous polarization, tilt angle and response time have been previously described.[24] Commercial switching cells were obtained from Displaytech (4 μm spacer, parallel rubbed, 0.25 $cm^2$ active area) and used for all electric field studies. Thermal polarized optical microscopy studies were conducted using an Olympus BX60 polarizing microscope used in conjunction with a Mettler FP82 HT hot stage controlled by a Mettler FP90 central processor.

X-Ray diffraction studies were performed on a Scintag $X_1$ diffraction system with a theta-theta powder diffractometer fitted with a solid state Si(Li) detector. The diffraction system was equipped with a Research Instruments heater controlled by a Micristar temperature processor. Scans were taken at 30 kV and 15 mA at a scan rate of approximately 0.5° $min^{-1}$. Samples were prepared by placing the solid material on a glass cover slip, heating to the isotropic phase to form a continuous film in the beam path, and then slowly cooling the material into the liquid crystalline phase.

## Synthesis

**Hex-5-enyl toluene-*p*-sulfonate.** A few crystals of potassium iodide were added to a mixture of toluene-*p*-sulfonyl chloride (32.44 g, 0.170 mol) in 60 ml dry pyridine. The solution was cooled to 0 °C under $N_2$ in a 250 ml round bottomed flask. Hex-5-en-l-ol (14.2 g, 0.142 mol) was added dropwise and the mixture was stirred at 0 °C for 4 h. The solution was diluted with 100 ml water and extracted with three 75 ml portions of diethyl ether. The organic fractions were combined and washed with dilute HCl, followed by water, and dilute NaOH. After a final water wash, the ethereal solution was dried over $MgSO_4$ and filtered. The solvent was evaporated under reduced pressure to yield 32.0 g (88%) of the desired tosylate as a clear oil. $^1$H NMR (ppm, $CDCl_3$): $\delta$ 1.40 (m, 2H, $CH_2$), 1.62 (m, 2H, $CH_2$), 2.00 (m, 2H, $CH_2$), 2.43 (s, 3H, $ArCH_3$), 4.02 (t, $J$ = 3.3 Hz, 2H, $OCH_2$), 4.96 (m, 1H, *Z* CH=$CH_2$), 5.15 (m, 1H, *E* CH=$CH_2$), 5.70 (m, 1H, CH=$CH_2$), 7.35 (d, $J$ = 6.6 Hz, 2H, ArH), 7.80 (d, $J$ = 6.6 Hz, 2H, ArH).

**Dec-9-enyl toluene-*p*-sulfonate.** The same procedure as above was employed with dec-9-en-l-ol (5.00 g, 32.0 mmol). Yield = 4.38 g (44%) clear oil. $^1$H NMR (ppm, $CDCl_3$): $\delta$ 1.20–1.40 (br m, 10H, $(CH_2)_5$), 1.60 (m, 2H, $CH_2$), 2.00 (m, 2H, $CH_2$), 2.43 (s, 3H, $ArCH_3$), 4.03 (t, $J$ = 3.6 Hz, 2H, $OCH_2$), 4.98 (m, 1H, *Z* CH=$CH_2$), 5.18 (m, 1H, *E* CH=$CH_2$), 5.80 (m, 1H, CH=$CH_2$), 7.38 (d, $J$ = 6.9 Hz, 2H, ArH), 7.80 (d, $J$ = 6.9 Hz, 2H, ArH).

**Methyl 4-(hex-5-enyloxy)benzoate.** Methyl 4-hydroxybenzoate (7.30 g, 0.048 mol) was dissolved in 100 ml dry DMF under $N_2$. The flask was chilled to 5 °C and anhydrous NaH (1.25 g, 0.052 mol) was added. The solution was stirred for 1 h and 11.00 g (0.043 mmol) hex-5-enyl toluene-*p*-sulfonate in 50 ml dry DMF was added dropwise over 30 min. The mixture was stirred for 1 h at room temperature, heated to 80 °C, and allowed to stir an additional 20 h. After cooling, the reaction mixture was diluted with 50 ml water. The organic phase was extracted with three 100 ml fractions of diethyl ether. This extract was washed with three 100 ml portions of 1 M HCl followed by three 100 ml portions of 10% $NaHCO_3$. After a final wash with saturated aqueous NaCl, the organic portions were dried over $MgSO_4$ and solvent was removed by rotary evaporation. The crude material was purified by column chromatography (eluent 2:1 hexanes–ethyl acetate) to yield 7.02 g (69%) of colorless oil. $^1$H NMR ($CDCl_3$): $\delta$ 1.60 (m, 2H, $CH_2$), 1.80 (m, 2H, $CH_2$), 2.13 (m, 2H, $CH_2$), 3.86 (s, 3H, $ArCH_3$), 4.00 (t, $J$ = 3.3 Hz, 2H, $CH_2O$), 5.02 (m, 1H, *Z* CH=$CH_2$), 5.22 (m, 1H, *E* CH=$CH_2$), 5.80 (m, 1H, CH=$CH_2$), 6.88 (d, $J$ = 7.2 Hz, 2H, ArH), 7.97 (d, $J$ = 7.2 Hz, 2H).

**Methyl 4-(oct-7-enyloxy)benzoate.** An analogous procedure as above was employed with 8-bromooct-1-ene (5.00 g, 26.2 mmol). Yield = 5.28 g (65%) of a colorless oil. $^1$H NMR (ppm, $CDCl_3$): $\delta$ 1.30–1.50 (m, 6H, $(CH_2)_3$), 1.80 (m, 2H, $CH_2$), 2.05 (m, 2H, $CH_2$), 3.88 (s, 3H, $ArCH_3$), 4.00 (t, $J$ = 3.3 Hz, 2H), 4.98 (m, 1H, *Z* CH=$CH_2$), 5.14 (m, 1H, *E* CH=$CH_2$), 5.80 (m, 1H, CH=$CH_2$), 6.91 (d, $J$ = 6.9 Hz, 2H, ArH), 7.97 (d, $J$ = 6.9 Hz, 2H, ArH).

**Methyl 4-(dec-9-enyloxy)benzoate.** An analogous procedure as above was employed with dec-9-enyl toluene-*p*-sulfonate (5.00 g, 16.1 mmol). Yield = 2.27 g (69%) of a colorless oil. $^1$H NMR (ppm, $CDCl_3$): $\delta$ 1.30–1.52 (br m, 10H, $(CH_2)_5$), 1.80 (m, 2H, $CH_2$), 2.08 (m, 2H, $CH_2$), 3.90 (s, 3H, $ArCH_3$), 4.02 (t, $J$ = 3.0 Hz, 2H, $CH_2O$), 5.00 (m, 1H, *Z* CH=$CH_2$), 5.16 (m, 1H, *E* CH=$CH_2$), 5.82 (m, 1H, CH=$CH_2$), 6.91 (d, $J$ = 6.6 Hz, 2H, ArH), 8.00 (d, $J$ = 6.6 Hz, 2H, ArH).

**4-(Hex-5-enyloxy)benzoic acid.** Methyl 4-(hex-5-enyloxy)-benzoate (6.90 g, 31.33 mmol) was dissolved in a mixture of 50 ml 5% aqueous KOH and 50 ml ethanol. The solution was heated to reflux and allowed to stir for 4 h. The mixture was cooled and the solvent removed to yield a white powder, which was recrystallized from acetic acid. The solid was redissolved in diethyl ether and washed repeatedly with water to remove traces of acid. After drying over $MgSO_4$, the solvent was removed by rotary evaporation to yield 5.40 g (82%) of white crystals. DSC (5 °C $min^{-1}$): K–N 99 °C, N–I 129 °C; *lit.*,[25] K–N 101 °C, N–I 141 °C; $^1$H NMR (ppm, $CDCl_3$): $\delta$ 1.52 (m, 2H, $CH_2$), 1.72 (m, 2H, $CH_2$), 2.16 (m, 2H, $CH_2$), 4.05 (t, $J$ = 3.0 Hz, 2H, $OCH_2$), 4.85 (m, 1H, *Z* CH=$CH_2$), 5.02 (m, 1H, *E* CH=$CH_2$), 5.81 (m, 1H, CH=$CH_2$), 7.05 (d, $J$ = 6.0 Hz, 2H, ArH), 7.92 (d, $J$ = 6.0 Hz, 2H, ArH).

**4-(Oct-7-enyloxy)benzoic acid.** The same procedure as above was used with methyl 4-(oct-7-enyloxy)benzoate (3.5 g, 13.3 mmol). Yield 2.61 g (76%) of white crystals. DSC (5 °C $min^{-1}$): K–S 81 °C, S–N 94 °C, N–I 137 °C; *lit.*,[25] K–S 78 °C, S–N 122 °C, N–I 139 °C; lit.,[26] K–S 82 °C, S–N 98 °C, N–I 140 °C. $^1$H NMR (ppm, $CDCl_3$): $\delta$ 1.45 (br m, 6H, $(CH_2)_3$), 1.79 (m, 2H, $CH_2$), 2.06 (m, 2H, $CH_2$), 4.02 (t, $J$ = 3.3 Hz, 2H, $OCH_2$), 4.95 (m, 1H, *Z* CH=$CH_2$), 5.12 (m, 1H, *E* CH=$CH_2$), 5.80 (m, 1H, CH=$CH_2$), 6.95 (d, $J$ = 6.9 Hz, 2H, ArH), 8.00 (d, $J$ = 6.9 Hz, 2H, ArH).

**4-(Dec-9-enyloxy)benzoic acid.** The same procedure as above was used with methyl 4-(dec-9-enyloxy)benzoate (1.4 g, 4.82 mmol). Yield 0.86 g (65%) of white crystals. DSC (5 °C $min^{-1}$): K–S 76 °C, S–N 108 °C, N–I 131 °C; *lit.*,[25] K–S 77 °C, S–N 116 °C, N–I 137 °C. $^1$H NMR (ppm, $CDCl_3$): $\delta$ 1.28–1.50 (br m, 10H, $(CH_2)_5$), 1.79 (m, 2H, $CH_2$), 2.04 (m, 2H, $CH_2$), 4.00 (t, $J$ = 3.0 Hz, 2H, $OCH_2$), 5.03 (m, 1H, *Z* CH=$CH_2$), 5.21 (m, 1H, *E* CH=$CH_2$), 5.80 (m, 1H, CH=$CH_2$), 6.95 (d, $J$ = 6.9 Hz, 2H, ArH), 8.01 (d, $J$ = 6.9 Hz, 2H, ArH).

**(*R*)-1-Methylheptyl 4′-[4-(hex-5-enyloxy)benzoyloxy]biphenyl-4-carboxylate (M-6).** A solution of 4-(hex-5-enyloxy)benzoic acid (0.573 g, 2.60 mmol) in dry dichloromethane (40 ml) was cooled to 0 °C under $N_2$ in a 100 ml round bottomed flask. DCC (0.590 g, 2.86 mmol) and DMAP (0.032 g,

0.26 mmol) were added and the solution was stirred for 30 min. (*R*)-1-Methylheptyl 4′-hydroxybiphenyl-4-carboxylate[24] (0.85 g, 2.60 mmol) was added slowly and the mixture was stirred for 24 h under $N_2$ at room temperature. After filtering out the white precipitate, the mixture was diluted with 100 ml $CH_2Cl_2$ and washed with three 50 ml portions of water, followed by 10% $NaHCO_3$ and saturated NaCl. This was then dried over $MgSO_4$ and the solvent was evaporated under reduced pressure. The residue was purified by column chromatography on silica gel (eluent: toluene) to yield 0.80 g (56%) of a white powder. $[\alpha]_D^{25} = -23.1$. $^1$H NMR (ppm, $CDCl_3$): $\delta$ 0.83 (t, 3H, $CH_3$), 1.20–1.40 (br m, 12H, $(CH_2)$), 1.50–1.70 (m, 3H), 1.80 (m, 2H), 2.11 (m, 2H), 4.02 (t, 2H), 5.00 (m, 1H, *Z* CH=$CH_2$), 5.15 (m, 1H, *E* CH=$CH_2$), 5.23 (m, 1H, CH), 5.80 (m, 1H, CH=$CH_2$), 6.95 (d, $J=6.6$ Hz, 2H, ArH), 7.33 (d, $J=6.6$ Hz, 2H, ArH), 7.62 (m, 4H, ArH), 8.20 (m, 4H, ArH). HRMS (CI+): $m/z=529.29$; Calc. for $C_{34}H_{40}O_5$: 529.30. Anal. Calc. for $C_{34}H_{40}O_5$: C, 77.24; H, 7.63. Found: C, 77.43; H, 7.63%.

**(*R*)-1-Methylheptyl 4′-[4-(oct-7-enyloxy)benzoyloxy]biphenyl-4-carboxylate (M-8).** 4-(Oct-7-enyloxy)benzoic acid (0.571 g, 2.30 mmol), (*R*)-1-methylheptyl 4′-hydroxybiphenyl-4-carboxylate[24] (0.750 g, 2.30 mmol) and DMAP (28.0 mg, 0.23 mmol) were charged to a dry 50 ml round bottomed flask and evacuated overnight. The flask was back filled with nitrogen, fitted with a rubber septum, and 20 ml dichloromethane was added *via* syringe. The solution was stirred for 10 min and 1-(3-(dimethylamino)propyl)-3-ethylcarbodiimide methiodide (EDC-$CH_3$I) (0.918 g, 3.09 mmol) was added dropwise as a 50% solution in dichloromethane. The mixture was stirred for 24 h at room temperature in a nitrogen flushed flask. After dilution in dichloromethane, the organic phase was washed sequentially with water, saturated sodium bicarbonate, and brine, and dried over $MgSO_4$. The solvent was evaporated and the residue was purified by column chromatography on silica gel (eluent: hexane–ethyl acetate 85:15) to yield 0.43 g (34%) of a white powder. $[\alpha]_D^{25} = -22.1$. $^1$H NMR (ppm, $CDCl_3$): $\delta$ 0.85 (t, 3H, $CH_3$), 1.38–1.60 (br m, 16H, $CH_2$), 1.67 (m, 5H, $CH_2$ and $CH_3$), 2.07 (m, 2H, $CH_2$), 4.00 (t, $J=3.6$ Hz, 2H, $OCH_2$), 5.02 (m, 1H, *Z* CH=$CH_2$), 5.14 (m, 1H, *E* CH=$CH_2$), 5.24 (m, 1H, CH), 5.80 (m, 1H, CH=$CH_2$), 7.00 (d, $J=6.6$ Hz, 2H, ArH), 7.32 (d, $J=6.6$ Hz, 2H, ArH), 7.65 (m, 4H, ArH), 8.17 (m, 4H, ArH). HRMS (CI+): $m/z=557.32$; Calc. = 557.33. Anal. Calc. for $C_{36}H_{44}O_5$: C, 77.67; H, 7.97. Found: C, 77.84; H, 8.00%.

**(*R*)-1-Methylheptyl 4′-[4-(dec-9-enyloxy)benzoyloxy]biphenyl-4-carboxylate (M-10).** The same procedure as used for **M-6** was employed with 4-(dec-9-enyloxy)benzoic acid (0.750 g, 2.71 mmol). Yield = 0.65 g (41%) of a white powder. $[\alpha]_D^{25} = -24.0$. $^1$H NMR (ppm, $CDCl_3$): $\delta$ 0.85 (t, $J=6.6$ Hz, 3H, $CH_3$), 1.20–1.40 (br m, 20H), 1.55–1.80 (br m, 5H, $CH_2$ and $CH_3$), 2.06 (m, 2H, $CH_2$), 4.03 (t, $J=6.0$ Hz, 2H, $OCH_2$), 4.97 (m, 1H, *Z* CH=$CH_2$), 5.17 (m, 1H, *E* CH=$CH_2$), 5.26 (m, 1H, CH), 5.79 (m, 1H, CH=$CH_2$), 6.97 (d, $J=7.2$ Hz, 2H, ArH), 7.27 (d, $J=7.2$ Hz, 2H, ArH), 7.63 (m, 4H, ArH), 8.13 (m, 4H, ArH). HRMS (CI+): $m/z=585.36$; Calc. = 585.36. Anal. Calc. for $C_{38}H_{48}O_5$: C, 78.05; H, 8.27. Found: C, 78.05; H, 8.34%.

### General procedure for hydrosilation of tetramethylcyclotetrasiloxane with olefin terminated mesogens:

**O-6.** (*R*)-1-Methylheptyl 4′-[4-(hex-5-enyloxy)benzoyloxy]-(*R*)-1-methylbiphenyl-4-carboxylate, **M-6** (0.806 g, 1.52 mmol) was charged to a dried 25 ml round bottomed flask and evacuated for 1 h. A septum was attached and the flask was purged with $N_2$. Dry toluene (5 ml) and 2,4,6,8-tetramethylcyclotetrasiloxane (85.2 mg, 0.354 mmol) were added by syringe. The solution was allowed to stir for 15 min. Dichloro(dicyclopentadienyl)platinum (1.5 mg) was added as a solution in toluene (1 mg ml$^{-1}$). The reaction was heated to 95 °C and stirred for 24 h. FTIR analysis of the solution (NaCl cell windows) showed the absence of a Si–H band at 2160 cm$^{-1}$, indicating the hydrosilation was complete. The reaction mixture was cooled to room temperature and the excess starting material was removed by repeated precipitation from toluene into methanol, until no trace of the compound could be detected by TLC. Residual platinum catalyst was removed by filtration of a toluene solution through a short column of diatomaceous earth (Dicalite Speed Plus, Acros). Removal of solvent by rotary evaporation afforded 0.67 g (83%) of a pale yellow powder. $^1$H NMR (ppm, $CDCl_3$): $\delta$ 0.092 (br s, 12H, $SiCH_3$), 0.59 (br m, 8H, $SiCH_2$), 0.90 (br m, 12H, $CH_3$), 1.31–1.84 (br m, 84H, $CH_2$ and $CH_3$), 4.06 (br m, 8H, $OCH_2$), 5.19 (br m, 4H, CH), 6.97 (br m, 8H, ArH), 7.29 (br m, 8H, ArH), 7.64 (br m, 16H, ArH), 8.15 (br m, 16H, ArH). FTIR (cm$^{-1}$, KBr) $\nu$ 1711 (C=O), 1731 (C=O), absence of 2160 (Si–H). HRMS (CI+): $m/z=2353.16$; Calc. = 2353.16. Anal. Calc. for $C_{140}H_{176}O_{24}Si_4$: C, 71.45; H, 7.54; Si, 4.77. Found: C, 71.58; H, 7.76; Si, 4.56%.

**O-8.** Yield = 67%. $^1$H NMR (ppm, $CDCl_3$): $\delta$ 0.11 (br s, 12H, $SiCH_3$), 0.57 (br m, 8H, $SiCH_2$), 0.91 (br m, 12H, $CH_3$), 1.25–1.89 (m, 100H, $CH_2$ and $CH_3$), 4.06 (br m, 8H, $OCH_2$), 5.19 (br m, 4H, CH), 7.00 (br m, 8H, ArH), 7.32 (br m, 8H, ArH), 7.66 (br m, 16H, ArH), 8.16 (br m, 16H, ArH). FTIR (cm$^{-1}$, KBr) $\nu$ 1711 (C=O), 1737 (C=O), absence of 2160 (Si–H). HRMS (CI+): $m/z=2466.29$; Calc. = 2466.29. Anal. Calc. for $C_{148}H_{192}O_{24}Si_4$: C, 72.01; H, 7.85; Si, 4.56. Found: C, 71.47; H, 7.21; Si, 5.11%.

**O-10.** Yield = 89%. $^1$H NMR (ppm, $CDCl_3$): $\delta$ 0.053 (br s, 12H, $SiCH_3$), 0.49 (br m, 8H, $SiCH_2$), 0.86 (br m, 12H, $CH_3$), 1.19–1.86 (m, 116H, $CH_2$ and $CH_3$), 3.99 (br m, 8H, $OCH_2$), 5.12 (br m, 4H, CH), 6.93 (br m, 8H, ArH), 7.28 (br m, 8H, ArH), 7.64 (br m, 16H, ArH), 8.10 (br m, 16H, ArH). FTIR (cm$^{-1}$, KBr) $\nu$ 1716 (C=O), 1731 (C=O), absence of 2160 (Si–H). Anal. Calc. for $C_{156}H_{208}O_{24}Si_4$: C, 72.61; H, 8.12; Si, 4.35. Found: C, 71.56; H, 8.14; Si, 5.08%.

## Results and discussion

### Synthesis

The synthesis of the alkenyl mesogens is outlined in Scheme 1. Olefin terminated alkyl ethers of methyl 4-hydroxybenzoate were prepared from the corresponding ω-bromide or tosylate with sodium hydride. Three lengths of the tethering carbon chain (6, 8, 10) were prepared. When an ω-halide was not commercially available, the tosylate was prepared from the parent alcohol and tosyl chloride. Saponification of the methyl esters with potassium hydroxide in aqueous ethanol afforded the carboxylic acids, all of which possessed liquid crystalline phases as determined by DSC. These acids were subsequently esterified with (*R*)-1-methylheptyl 4′-hydroxybiphenyl-4-carboxylate, the synthesis of which is reported elsewhere.[24] Mild dehydrating reagents (DCC and EDC-MeI) brought about these transformations. DSC and thermal polarized optical microscopy (TPOM) analyses provided evidence of various smectic phases in these materials.

The cyclic oligomeric siloxanes were prepared by hydrosilation of olefin terminated smectogens with a well-defined polyfunctional cyclic hydrosiloxane, 2,4,6,8-tetramethylcyclotetrasiloxane.[27–30] This transformation is brought about with a Pt(II) catalyst, dichloro(dicyclopentadienyl)platinum.[31] Progress of the reaction was monitored by FTIR spectroscopy, as a decrease in intensity of the Si–H band at ~2160 cm$^{-1}$ is easily detectable as hydrosilation occurs. Removal of residual

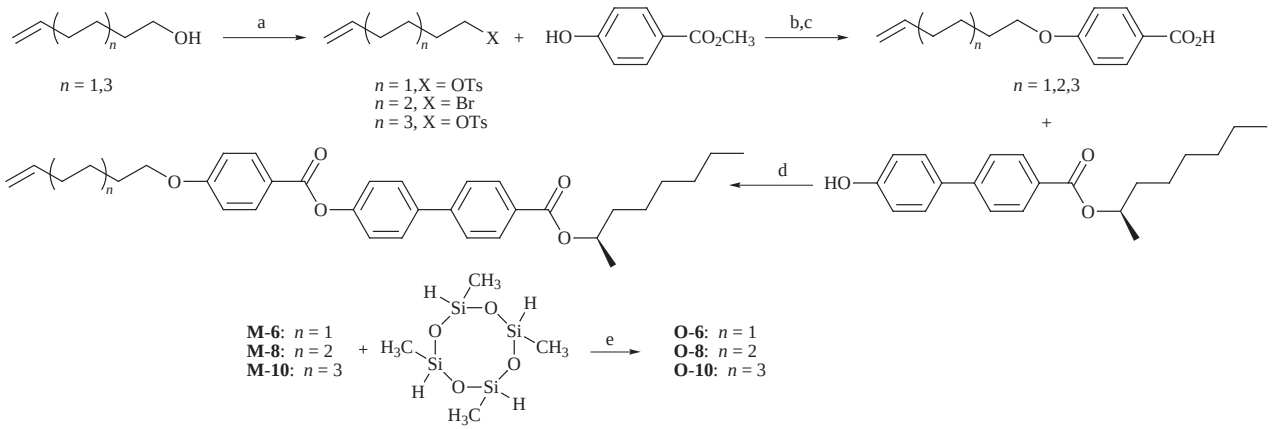


**Scheme 1** Synthesis of olefin terminated smectogens and hydrosilation to cyclic siloxane oligomers: a: TsCl, Pyr; b: NaH, DMF; c: KOH, $H_2O$, $CH_3CH_2OH$; d: DCC–DMAP or EDC-MeI, THF; e: DCDCPt, Tol.

catalyst was done effectively by filtration through diatomaceous earth. Characterization by FTIR, $^1$H NMR, HRMS and elemental analysis provided proof of structure and purity.

### Thermal analysis

Differential scanning calorimetry provided preliminary indication of phase transitions in both the monomeric olefins (**M**-series) and the cyclic oligomers (**O**-series). A DSC thermogram of **M-10** is shown in Fig. 2. This thermogram is typical for the monomeric compounds in that large, first order transitions are evident for transitions between the crystal and liquid crystal states and the liquid crystal to isotropic states only upon heating. The recrystallization transition to crystal is lacking on the cooling cycles, resulting in super-cooled material at this scan rate ($5\,^{\circ}C\,min^{-1}$). Upon close inspection, low enthalpy transitions corresponding to mesophasic transitions are identifiable. These become more apparent when the liquid crystalline temperature range is expanded, as in Fig. 3.

DSC of the oligomeric compounds showed similar, but less defined transitions than their monomeric analogs. Additionally, the liquid crystalline phases are broadened in the oligomers, but the polymorphism is reduced. For example, **O-10** showed only two transitions over the temperature range investigated (K-LC, LC-I), while the monomeric **M-10** distinctly showed four transitions. TPOM allowed for phase assignments to be made and further distinguished the low molecular mass compounds from the oligomers.

### Thermal polarized optical microscopy

Identification of mesophases and transition temperatures was conducted by examining the texture of a thin liquid crystal film sandwiched between untreated glass substrates.[32] To prepare a sample for observation, the liquid crystal was heated to the isotropic phase on a clean glass slide. A cover slip is then placed onto the glass slide and positioned so it was in contact with the isotropic material, at which point the liquid crystal was drawn between the slide and the cover slip by capillary forces, forming a thin film. The material was then slowly cooled into the highest temperature liquid crystal phase. The polymorphism of the monomers and oligomers, as determined by a combination of DSC and TPOM, is summarized in Table 1 and is graphically represented in Fig. 4.

The $S_A$* phase of the monomers exhibited both focal conic and homeotropic textures when viewed between crossed polar-

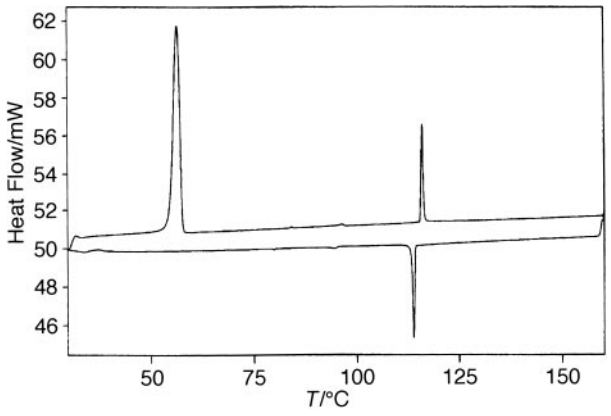


**Fig. 2** DSC thermogram of **M-10**.

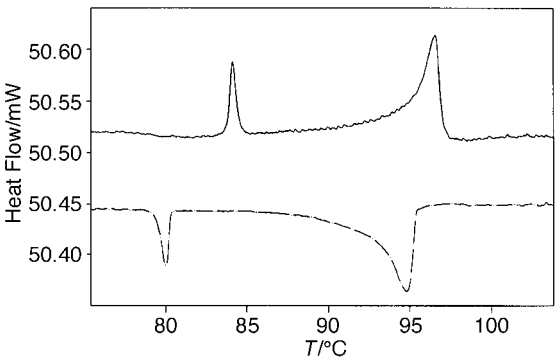


**Fig. 3** Expanded DSC thermogram of **M-10** showing mesophasic transitions.

**Table 1** Phase assignments, transition temperatures/°C, and transition enthalpies/J $g^{-1}$ as determined by TPOM and DSC

| | | | | | | | | | | |
|---|---|---|---|---|---|---|---|---|---|---|
| **M-6:** | K | 65 °C / 44.3 J $g^{-1}$ | $S_A$* | 124 °C / 8.89 J $g^{-1}$ | I | | | | | |
| **M-8:** | K | 61 / 37.8 | $S_{CA}$* | 67 / 0.06 | $S_C$* | 84 / 0.17 | $S_A$* | 120 / 8.50 | I | |
| **M-10:** | K | 56 / 55.4 | $S_{CA}$* | 84 / 0.08 | $S_C$* | 97 / 0.43 | $S_A$* | 116 / 8.18 | I | |
| **O-6:** | K | <25 | $S_A$* | 119 / 7.48 | I | | | | | |
| **O-8:** | K | 35 / 1.63 | $S_C$* | 148 / 6.02 | I | | | | | |
| **O-10:** | K | 38 / 4.35 | $S_C$* | 160 / 4.98 | I | | | | | |

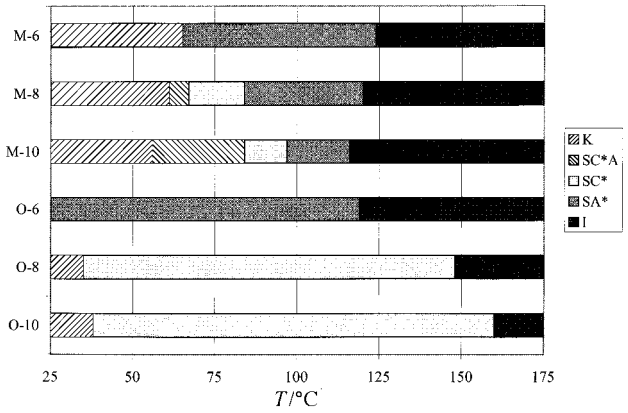


**Fig. 4** Polymorphism of monomeric (**M-#**) and oligomeric (**O-#**) compounds.

izers. The focal conic texture of the $S_A$* phase of **M-10** is shown in Fig. 5. The homeotropic region remained extinct when viewed in either reflected or transmitted light. Cooling of the monomers resulted in a transition to a $S_C$* phase for **M-8** and **M-10**, while **M-6** only exhibited a $S_A$* mesophase. The transition to the $S_C$* phase was evident by the formation of pitch lines (arcs) in the focal conic texture, which breaks apart to form the broken focal conic characteristic of tilted smectics. The banded, broken focal conic texture of the $S_C$* phase of **M-10** is shown in Fig. 6. Also, the homeotropic region of the same material viewed in reflected light showed an iridescent texture resulting from the formation of a helical structure.[33] The color of the texture changed with temperature, indicating a temperature dependent helical pitch. This iridescent texture is shown in Fig. 7. Further cooling led to the formation of an antiferroelectric ($S_{CA}$*) phase for both **M-8** and **M-10**. The transition from $S_C$* to $S_{CA}$* was noted by the loss of the iridescent texture (reflected light) in the homeotropic regions and the formation of a dark, planar texture. Hence, the pitch of the antiferroelectric helix is outside the wavelength range of the visible spectrum. No photomicrographs of this phase are presented because the homeotropic texture was indiscernible in the reproduction and no change was evident in the focal conic regions.

TPOM of the oligomeric species did not provide conclusive phase assignments. Very small domains formed when the materials were slowly cooled from the isotropic to the liquid crystalline state. The texture appeared to be focal conic, with no homeotropic regions forming in the thin film. The materials

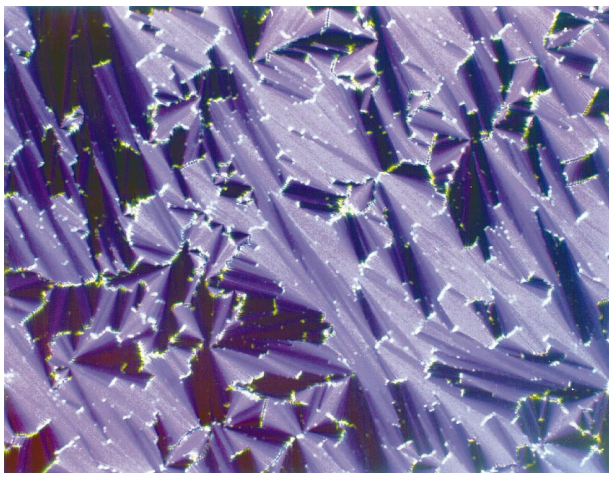

**Fig. 5** Photomicrograph of the focal conic texture of the $S_A$* phase of **M-10** at 110 °C. Magnification = 75 × .

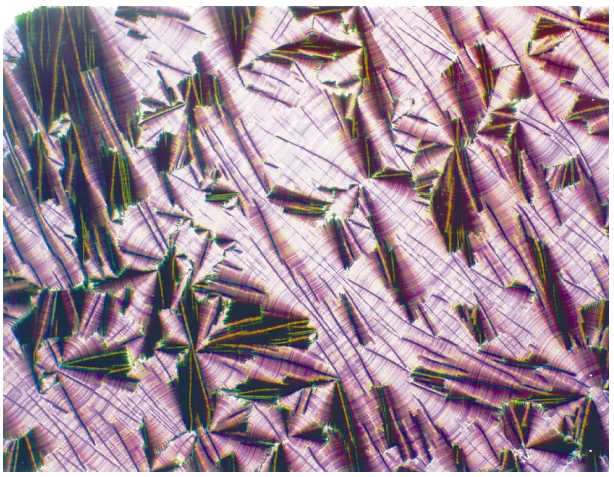

**Fig. 6** Photomicrograph of the banded, broken focal conic texture of the $S_C$* phase of **M-10** at 90 °C. Magnification = 75 × .

could be classified as smectic, but the domains were too small to closely examine the texture. Thus, no determination could be made concerning the condition of the fan structure or the presence of pitch lines. However, from electrooptic studies, phase assignments of the three oligomers were made.

For both the monomers and oligomers, an alkyl chain length consisting of six carbons only produces a $S_A$*. Increasing the length of the chain to eight or ten carbons produces both ferroelectric and antiferroelectric phases in the monomers and a ferroelectric phase in the oligomers. It is particularly interesting to note that the ferroelectric phases of **O-8** and **O-10** exist over a temperature range of approximately 120 °C! It was also found that increasing the chain length in the monomers decreases both the clearing point and the crystallization temperature. The opposite trend is true for the oligomers—increased chain length results in increased transition temperatures. These trends are clearly discernible in Table 1.

### Electro-optic studies

The polarizations of the ferroelectric (and antiferroelectric) phases of these materials were measured using the triangular wave method with a field of 45 V $\mu m^{-1}$ at 1 Hz.[24,34] There is some degree of error associated with the measurements of the oligomers, due to the estimation of the active electrode area.

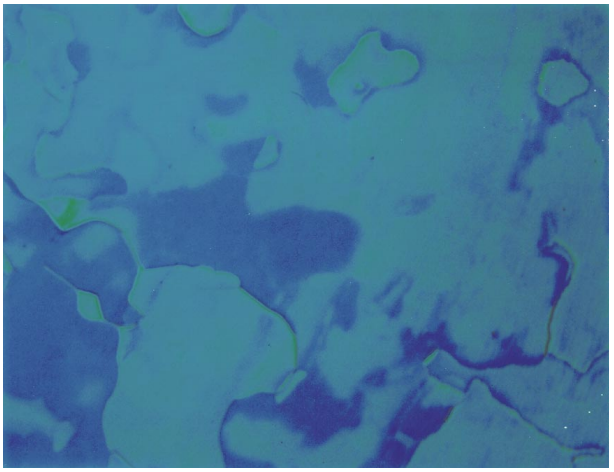

**Fig. 7** Photomicrograph of the iridescent homeotropic texture of the $S_C$* phase of **M-10** viewed with reflected light at 90 °C. Magnification = 75 × .

To fill the switching cells, the compounds were heated to the isotropic state, placed at the opening of the cells, and the gap was allowed to fill by capillary flow. The monomeric compounds completely filled the cells while this was not achievable with the oligomers due to their high viscosity. The active area of the partially filled cells was estimated optically using the response time measurement system consisting of a laser, the sample cell, a crossed polarizer and a photodiode in series. This was accomplished by measurement of the ratio of the amount of transmitted light to extinguished light with the samples in or near their crystalline state at room temperature. This area was estimated for each oligomeric compound independently and reproducible values were attainable with $\sim 5\%$ variance.

The polarizations of the ferroelectric compounds (**M-8**, **M-10**, **O-8**, and **O-10**) are compared in Fig. 8. The polarization values are comparable to but slightly higher than those of previously reported systems with like architectures.[4] For a chiral, tilted molecule, the magnitude of the spontaneous polarization is dependent on the tilt angle of the director, the strength of the dipole moment orthogonal to the director, and the degree of steric hindrance to rotation about the long axis of the molecule.[35,36] Increasing the alkyl chain length does not appear to strongly affect these properties, and thus, no marked change in polarization is seen between **M-8** and **M-10** and for **O-8** and **O-10**. The ferroelectric switching observed at low temperatures is possibly the result of a field induced supercooled region, and that would explain the apparent inconsistency between the electrooptic analyses and the DSC data.

Also of note in Fig. 8 are the similar polarizations of the monomers and those of the oligomers, especially when correlated with tilt angle measurements. Tilt angles were measured to $\pm 1^\circ$ by applying a square wave voltage and rotating the sample to a state of maximum extinction. The position of the stage is noted and the field is reversed. The stage is rotated again to maximum extinction and the angle between the positions is divided in half. One normally expects increased polarization to correspond closely with tilt angle values and thus similar tilt angles would be expected for the monomers and oligomers in this series. However, examination of their tilt angles shows dramatically different values. **M-8** and **M-10** exhibit the typical behavior of increasing tilt angle with decreasing temperature with maximum values, measured near crystallization temperature, of 26.5° and 27.5° respectively; whereas, the tilt angles of **O-8** and **O-10** were determined to be 9.5° and 10° respectively and nearly temperature independent. While these may appear to be conflicting data, this phenomenon may be caused by restricted rotation of the smectogens resulting from attachment to the cyclic backbone.

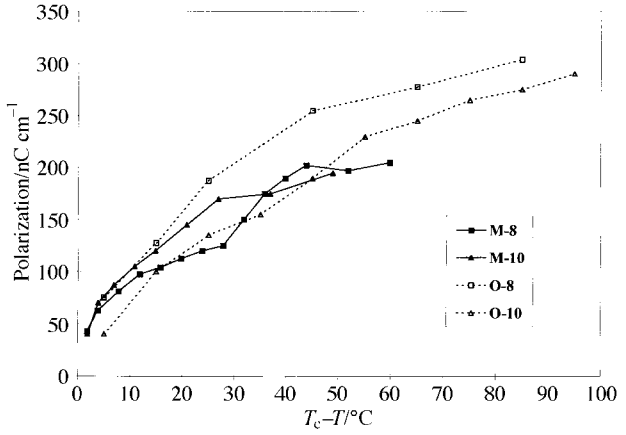


**Fig. 8** Polarization response of the monomers and oligomers. $T_c - T$ is the reduced temperature where $T_c$ is the transition temperature from $S_A$* to $S_C$*.

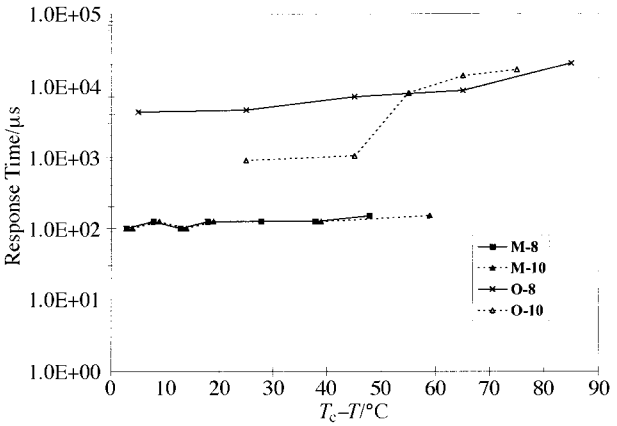


**Fig. 9** Response time of the monomers and oligomers.

It is proposed that in this environment, the restricted rotation and reduced flexibility result in some degree of dipole alignment that compensates for the decreased tilt angle in terms of polarization. Furthermore, microphase separation of cyclic siloxane LC's has been reported and may contribute to the degree of orientation in these systems.[37] Influence of restricted topology on molecular orientation of this type is the topic of recent treatises by Goodby and coworkers.[18,37]

The temperature dependent response times for **M-8**, **M-10**, **O-8** and **O-10** are shown in Fig. 9. The response time measured was the total response time, equal to the sum of the lag time and switch time. It should be noted that some of these measurements were made in a supercooled state, during which there exists the possibility for a phase transition. However, during direct observation by TPOM, no crystallization was detected. This is an important observation in light of the somewhat unexpected results of these measurements. As expected because of their inherently higher viscosity, the response time is larger for the oligomers than for the monomers. Although only made up of four mesogenic units, the oligomers unfortunately exhibit response times similar to higher molecular weight polymeric side chain FLC's.[38] These data reveal nearly identical response times for both **M-8** and **M-10**, increasing slightly from 100 μs to 150 μs, as the temperature is reduced. Increasing the length of the alkyl chain of the oligomers has a more pronounced effect on response times. **O-10** shows a larger range of response time, switching as much as five times faster than **O-8** at higher temperatures, but exhibiting slower response times at temperatures nearer to the crystalline state. It may be that above a critical spacer chain length (**O-10** *vs.* **O-8**), a threshold of rotational freedom is reached that affords a greater temperature dependence on the switching time, but this is tenuous to assert without more data. The response time $\tau$ of a FLC is related to the torsional, or bulk, viscosity $\eta$ as shown in eqn. (1),

$$\tau \cong \eta/(EP_s) \quad (1)$$

where $E$ is the electric field and $P_s$ is the spontaneous polarization.[39] The spontaneous polarizations were nearly the same for the two materials and the electric field used was held constant for both measurements. Therefore, the data suggest a variance in the torsional viscosity is responsible for the different response times of **O-10** compared to **O-8** at reduced temperatures below 50 °C. The addition of the two extra carbons in the alkyl chain of **O-10** apparently provides the increased flexibility of the molecular structure required to reduce the effective viscosity and thereby lower the response time. This effect is not seen in the monomeric units, which have much less restriction to molecular movement and significantly lower bulk viscosities.

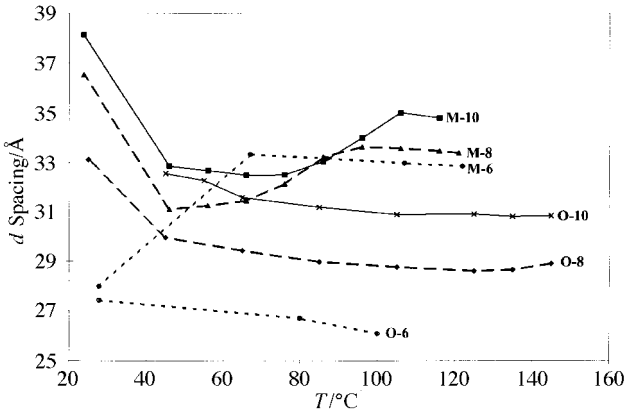


**Fig. 10** Temperature dependence of layer spacing for all six compounds. The layer spacing is taken to be the measured *d* spacing from small angle X-ray diffraction.

### X-Ray investigations

Layer spacing of the smectic materials was determined by small angle X-ray diffraction and is shown in Fig. 10. For each scan, the *d* spacing of the smallest angle diffraction was assumed to be smectic layer spacing. The layer spacing of **M-6** is nearly constant, consistent with a $S_A$* phase, until crystallization occurs below 65 °C. **M-10** and **M-8** show fixed layer thickness above their Curie temperatures ($T_c$) and decreased layer spacing with cooling, resulting from an increase in the molecular tilt. In the $S_A$* phase, the monomers exhibit the expected trend with **M-10** possessing the longest layer and **M-6**, the shortest. Upon crystallization, **M-10** and **M-8** show dramatic increases in layer spacing, while **M-6** shows a sharp decrease in this value. These abrupt disclinations are likely due to crystallization occurring in the samples. While a supercooled regime was detected in the DSC analysis, the static nature of the X-ray diffraction experiment and the confines of the sample cell may induce crystallization in these samples at a different temperature. Single crystal analysis would shed light on the different packing arrangement of **M-6** compared to the other two monomers to account for this observation. However, we were unable to grow single crystals of these materials using conventional methods.

The oligomers also follow the expected trend with **O-10** having the greatest layer thickness followed by **O-8** and **O-6** respectively. The layer spacings were nearly independent of temperature which is consistent with the nearly constant tilt angles measured for the $S_C$* phases of **O-8** and **O-10**. Higher *d* spacings were measured upon crystallization for **O-8** and **O-10**, while **O-6** remained liquid crystalline at room temperature.

The layer spacing of each monomer was found to be greater than that of the corresponding oligomer. The layer spacing of the monomers in the $S_A$* phase compares well to the predicted end to end length of the monomers (within 10%) obtained using space filling molecular models, as shown in Table 2. This

**Table 2** Layer spacings as determined by X-ray diffraction and predicted end-to-end dimensions as determined using space filling molecular models

| | Spacing/Å | |
|---|---|---|
| | Measured | Predicted |
| **M-6** | 32.8 | 33.6 |
| **M-8** | 33.1 | 35.4 |
| **M-10** | 34.9 | 37.3 |
| **O-6** | 25.9 | |
| **O-8** | 28.9 | |
| **O-10** | 31.3 | |

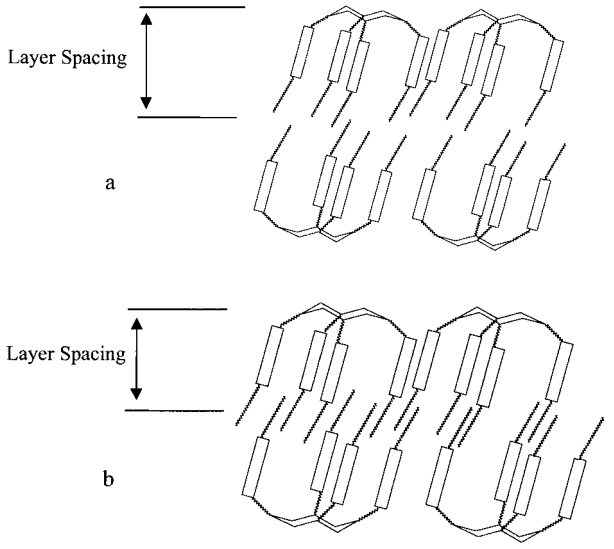


**Fig. 11** Schematic representation of possible molecular arrangements resulting in different layer spacings: a: discrete monolayer arrangement; b: interdigitation of mesogens.

suggests a smectic ordering of the monomers to be produced by a monolayer arrangement; that is, mesogens are completely contained within one layer. The smaller layer spacing measured for the oligomers is possibly the result of interdigitation occurring in the layers as proposed schematically in Fig. 11. Other researchers working with similar systems have proposed comparable intercalated arrangements.[37,40] This interdigitation could effectively reduce the layer spacing below that which is found for the mesogens alone, accounting for the smaller *d* spacing found in the X-ray diffraction patterns.

## Conclusions

Vinylic monomer units of different lengths have been attached to a ringed siloxane backbone. Two of the monomer units exhibit both ferroelectric and antiferroelectric ordering while their corresponding oligomers show only a ferroelectric phase, stable over the entire liquid crystalline temperature range. Electric field studies have shown the polarization of the monomers and oligomers to be approximately the same with no substantial dependence on chain length. The response times of the oligomers are more than an order of magnitude greater than the monomers. Increasing the chain length decreases the response time of the oligomers, but has little effect for the monomers, indicating that the viscosity of the oligomers is more strongly affected by the length of the alkyl chain. X-Ray diffraction studies have shown the length of the layer decreases as the alkyl chain length is decreased. Also, the monomers have greater layer spacing than the corresponding oligomers consistent with an interdigitated, bilayer packing arrangement of the oligomers.

## Acknowledgements

We would like to thank Dr Steven Swinnea and Dr Hugo Steinfink for their assistance in gathering X-ray diffraction data. DRM would like to thank the Eastman Kodak Company for providing him with a fellowship. Partial funding for this research was provided by the Robert A. Welch Foundation.

## References

1 H. Finkelmann, H. Ringsdorf, W. Siol and J. H. Wendorff, in *Mesomorphic Order in Polymers and Polymerizations in Liquid*

*Crystal Media*, ed. A. Blumstein, American Chemical Society, Washington, DC, 1978.
2 H. Finkelmann, M. Happ, M. Portugall and H. Ringsdorf, *Makromol. Chem.*, 1978, **179**, 2541.
3 V. Percec and H. Oda, *J. Polym. Sci.*, *Part A: Polym. Chem.*, 1995, **33**, 2359.
4 H. Poths, E. Wischerhoff, R. Zentel, A. Schönfeld, G. Henn and F. Kremer, *Liq. Cryst.*, 1995, **18**, 811.
5 R. D. C. Richards, W. D. Hawthorne, J. S. Hill, M. S. White, D. Lacey, J. A. Semlyn, G. W. Gray and T. C. Kendrick, *J. Chem. Soc.*, *Chem. Commun.*, 1990, 95.
6 I. Nishiyama and J. W. Goodby, *J. Mater. Chem.*, 1993, **3**, 169.
7 E. Wischerhoff and R. Zentel, *Macromol. Chem. Phys.*, 1994, **195**, 1593.
8 G.-H. Hsiue, K.-R. Lee and J.-H. Chen, *Macromol. Chem. Phys.*, 1995, **196**, 2601.
9 A. Kocot, R. Wrzalik, J. K. Vij and R. Zentel, *J. Appl. Phys.*, 1994, **75**, 728.
10 G. Decher, J. Reibel, M. Honig, I. G. Voigt-Martin, A. Dittrich, H. Ringdorf, H. Poths and R. Zentel, *Ber. Bunsen-Ges. Phys. Chem.*, 1993, **97**, 1386.
11 M. Svensson, B. Helgee, K. Skarp and G. Andersson, *J. Mater. Chem.*, 1998, **8**, 353.
12 G.-H. Hsiue and J.-H. Chen, *Macromolecules*, 1995, **28**, 4366.
13 K. D. Gresham, C. M. McHugh, T. J. Bunning, R. L. Crane, H. E. Klei and E. T. Samulski, *J. Polym. Sci.*, *Part A: Polym. Chem.*, 1994, **32**, 2039.
14 C. McHugh, D. W. Tomlin and T. J. Bunning, *Macromol. Chem. Phys.*, 1997, **198**, 2387.
15 K. Grüneberg, J. Naciri and R. Shashidhar, *Chem. Mater.*, 1996, **8**, 2486.
16 K. D. Gresham, C. M. McHugh, T. J. Bunning, H. E. Klei, E. T. Samulski and R. L. Crane, *Polym. Prepr.* (*Am. Chem. Soc.*, *Div. Polym. Chem.*), 1993, **35**, 697.
17 D. M. Walba, D. A. Zummach, M. D. Wand, W. N. Thurmes, K. M. More and K. E. Arnett, *Proc. SPIE*, *Int. Soc. Opt. Eng.*, 1993, **1911**, 21.
18 G. H. Mehl and J. W. Goodby, *Angew. Chem.*, *Int. Ed. Engl.*, 1996, **35**, 2641.
19 J. W. Goodby, G. H. Mehl, I. M. Saez, R. P. Tuffin, G. Mackenzie, R. Auzély-Velty, T. Benvegnu and D. Plusquellec, *Chem. Commun.*, 1998, 2057.
20 S. G. McNamee, T. J. Bunning, S. S. Patnaik, C. M. McHugh, C. K. Ober and W. W. Adams, *Liq. Cryst.*, 1995, **18**, 787.
21 K. B. Wagener, F. Zuluga and S. Wanigatunga, *Trends Polym. Sci.*, 1996, **4**, 157.
22 Q. Wang, H. Zhang, G. K. S. Prakash, T. E. Hogen-Esch and G. A. Olah, *Macromolecules*, 1996, **29**, 6691.
23 J. W. Goodby, J. S. Patel and E. Chin, *J. Mater. Chem.*, 1992, **2**, 197.
24 D. R. Medeiros, M. A. Hale, J. K. Leitko and C. G. Willson, *Chem. Mater.*, 1998, **10**, 1805.
25 S. M. Kelly and R. Buchecker, *Helv. Chim. Acta*, 1988, **71**, 461.
26 C. Lin, P. Cheng and A. Blumstein, *Mol. Cryst. Liq. Cryst. Sci. Technol.*, *Sect. A*, 1995, **258**, 173.
27 J. Naciri, J. Ruth, G. Crawford, R. Shashidhar and B. R. Ratna, *Chem. Mater.*, 1995, **7**, 1397.
28 J. Newton, H. Coles, P. Hodge and J. Hannington, *J. Mater. Chem.*, 1994, **4**, 869.
29 J. Ojima, in *The Chemistry of Organic Silicon Compounds*, ed. S. Patai and Z. Rappoport, Wiley, New York, 1989, pp. 1479–1526.
30 J. K. Stille and D. B. Fox, *J. Am. Chem. Soc.*, 1970, **92**, 1274.
31 D. Drew and J. R. Doyle, in *Inorganic Syntheses*, ed. F. A. Cotton. McGraw-Hill, New York, 1971, vol. XIII, p. 47.
32 G. W. Gray and J. W. Goodby, *Smectic Liquid Crystals, Textures and Structures*, Hill, London, 1984.
33 I. Nishiyama, E. Chin and J. W. Goodby, *J. Mater. Chem.*, 1993, **3**, 161.
34 K. Miyasato, S. Abe, H. Takezoe, A. Fukuda and E. Kuze, *Jpn. J. Appl. Phys.*, 1983, **22**, L661.
35 R. B. Meyer, L. Liebert, L. Strzelecki and P. Keller, *J. Phys.* (*Paris*), 1975, **36**, 69.
36 J. S. Patel and J. W. Goodby, *Mol. Cryst. Liq. Cryst.*, 1987, **144**, 117.
37 G. H. Mehl and J. W. Goodby, *Chem. Ber.*, 1996, **129**, 521.
38 K. M. Blackwood, *Science*, 1996, **273**, 909.
39 S. T. Lagerwall and I. Dahl, *Mol. Cryst. Liq. Cryst.*, 1984, **114**, 151.
40 A. E. Blatch, I. D. Fletcher and G. R. Luckhurst, *Liq. Cryst.*, 1995, **18**, 801.

*Paper 8/09842E*